

## Salt Effect on the Photoelectron Emission Threshold from the Wet Surface of TiO<sub>2</sub>

S. Hitaka, K. Tomita, T. Ishioka and A. Harata

*Molecular and Material Sciences, Kyushu University, Kasugakoen 6-1, Kasuga, Fukuoka 816-8580, Japan*

### Introduction

Titanium oxide (TiO<sub>2</sub>) has attracted much interest for its unique characteristics of photocatalytic ability such as oxidation of organic compounds without any harmful oxidizing agent. It is widely applied to decompose various organic wastes with solar energy by illuminating the pollutant-adsorbed surface of TiO<sub>2</sub>. Though some wastewater treatment systems with TiO<sub>2</sub> have already been developed, their application to seawater is limited because salt in the seawater usually affect the photocatalytic reaction.

Makita *et al.* [1] reported enhanced photocatalytic reactions in aqueous solutions containing dilute inorganic salt. It is essential to understand salt-enhancement or suppression mechanism to apply photocatalytic reaction for seawater treatment. However, it is still obscure and precise analysis on the mechanism is needed.

In this report, threshold photon energy was measured on photoelectron emission process on the surface of wet TiO<sub>2</sub> containing salts. From the results, electronic structures on the TiO<sub>2</sub> surfaces were analyzed.

### Experimental

Monochromated synchrotron light (4-8) was emitted from the beamline chamber to a He-purged cell through an MgF<sub>2</sub> window. The emitted light was reflected on an Al mirror and vertical irradiated on the sample surface through a Cu-mesh electrode. The electrode was set above the wet TiO<sub>2</sub> surface and high voltage (400 V) was applied to the electrode. The emitted electron was trapped to the electrode and the total current was monitored by a picoammeter.

The sample was prepared by spreading TiO<sub>2</sub> powder (Degussa P-25, anatase:rutile = 8:2) on filter paper covering the bottom of a Pt cell and aqueous salt solution was added to the cell with the volume enough to keep all the powder wet. The salt concentration was 5 mM.

Threshold energy value was derived from the mathematical fitting of empirical formula:

$$S(\nu) = \sum S_i (h\nu - E_{th,i})^n \quad (1)$$

where  $S(\nu)$  is total signal intensity and  $E_{th,i}$  is the threshold energy of the  $i$ th component. As for index number,  $n = 2$  was used in analogy with the case of metal substrates.

### Results and Discussion

Photon energy dependence of the photoelectron intensity is shown in Fig. 1. The intensity is well fitted by formula (1) with single component and

derived threshold energy is listed in Table 1. The threshold energy for wet TiO<sub>2</sub> with no salt is 5.20 eV. As for single crystalline TiO<sub>2</sub>(111), the threshold energy is reported to be 5.1 eV. Since single crystal (111) surface is dominant for the used TiO<sub>2</sub> powder, it is considered the presence of moisture at the surface has little effect on the band structure of TiO<sub>2</sub>.

The threshold energy is clearly dependent on the salt species. The threshold value order of cation  $Mg^{2+} \sim Li^+ < Na^+ < no\ salt$  agrees well with the reversed order of photocatalytic activity. Smaller threshold suggests narrower band gap for the surface. The narrower band gap would improve the efficiency of photoexcitation because photons with weak energy become available for excitation.

From above discussion, it is considered that the enhancement by the salt is originated from the distortion of the valence band structure of TiO<sub>2</sub>. The result can be applied to evaluate photocatalytic activity before actual long-term photochemical experiments.

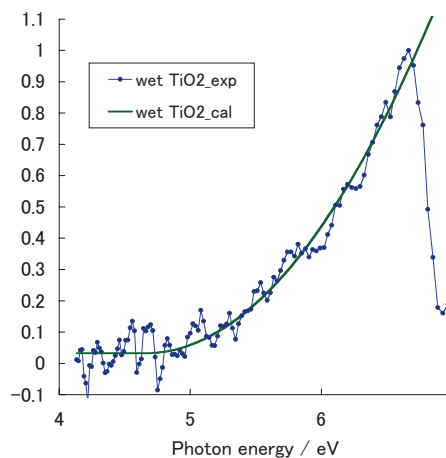


Fig. 1. Photon energy dependence on photoelectron intensity from wet TiO<sub>2</sub> surface.

Table 1. Salt dependence on the threshold energy of photoelectron emission from wet TiO<sub>2</sub>.

Substrate	Threshold / eV
TiO <sub>2</sub>	5.20
TiO <sub>2</sub> + 5 mM LiNO <sub>3</sub>	4.72
TiO <sub>2</sub> + 5 mM NaNO <sub>3</sub>	5.02
TiO <sub>2</sub> + 5 mM Mg(NO <sub>3</sub> ) <sub>2</sub>	4.71

[1] M. Makita and A. Harata, Chem. Eng. Proc. **47** (2008) 859.

## Development of Lower Environmental Load and UVSOR Exciting Luminescence Materials Using with Biomaterials Prepared by Soft Chemistry

M. Ohta

*Department of Material Science and Technology, Faculty of Engineering, Niigata University, Niigata 950-2181, Japan*

It was known that rare earth ions dosed for oral administration to mouse and rat are transferred to blood vessel through the ileum and deposited its teeth and bone, which mainly consists of hydroxyapatite ( $\text{Ca}_{10}(\text{PO}_4)_6(\text{OH})_2$ ) [1, 2]. Recently, rare earth is also useful as a contrast medium for magnetic resonance imaging, restriction enzyme, biocatalyst, and so on in fields of biochemistry, physiology, medicine, etc. However, the behavior of rare earth in the living body system remains an open question until now. We have found that Eu ion substituted Ba ion in Eu doped  $\text{Ba}_{10}(\text{PO}_4)_6\text{Cl}_2$  phosphor, which matrix is apatite structure [3]. The rare earth ion is also found to substitute easily for calcium ion in hydroxyapatite which is soaked in rare earth chloride aqueous solution, and to play on emission center.

In this study, hydroxyapatite samples doped with rare earth phosphate were prepared in order to apply to phosphor. Their characteristics were investigated by photoluminescent property of rare earth ion-doped hydroxyapatite samples excited by ultraviolet synchrotron orbital radiation light.

Eu-doped hydroxyapatite and Gd-doped hydroxyapatite samples were prepared as follows: hydroxyapatite was added with  $\text{EuPO}_4$  or  $\text{GdPO}_4$  and mixed homogeneously, and then heated at 1373 K for 1 hr.  $\text{EuPO}_4$  or  $\text{GdPO}_4$  was prepared by reaction of  $\text{GdCl}_3$  or  $\text{YbCl}_3$  and  $\text{Na}_3\text{PO}_4 \cdot 12\text{H}_2\text{O}$  and then fired at 1373 K for 1 hr.  $\text{GdCl}_3$  or  $\text{YbCl}_3$  was prepared by reaction of  $\text{Eu}_2\text{O}_3$  or  $\text{Gd}_2\text{O}_3$  and HCl.

The photoluminescent property of each sample excited by ultraviolet synchrotron orbital radiation light (BL1B) was detected by using with a multi-channel analyzer.

Figure 1 shows photoluminescence spectra of rare earth ion-doped hydroxyapatite samples excited by BL1B.

The data of X-ray powder diffraction indicated that the rare earth ion substituted for calcium ion in hydroxyapatite.

Figure 1 shows the photoluminescent spectra of Eu ion or Gd ion-doped hydroxyapatite samples excited by ultraviolet synchrotron orbital radiation light. Eu ion-doped sample emitted strong peaks due to f-f transition of  $\text{Eu}^{3+}$  and Gd ion-doped sample emitted a very strong peak due to f-f transition of  $\text{Gd}^{3+}$  by excitation from 10 nm to 100 nm. These strong emission phenomena due to rare earth ion suggest to the origin of multiphoton excitation.

[1] S. Hirano and K. T. Suzuki, Environ. Health Perspect. **104** (Supplement 1) (1996) 85.

[2] K. Kostial, B. Kargacin and M. Lendeka, Int. J. Radiat. Biol. Relat. Stud. Phys. Chem. Med. **51** (1987) 139.

[3] M. Sato, T. Tanaka and M. Ohta, J. Electrochem. Soc. **141** (1994) 1851.

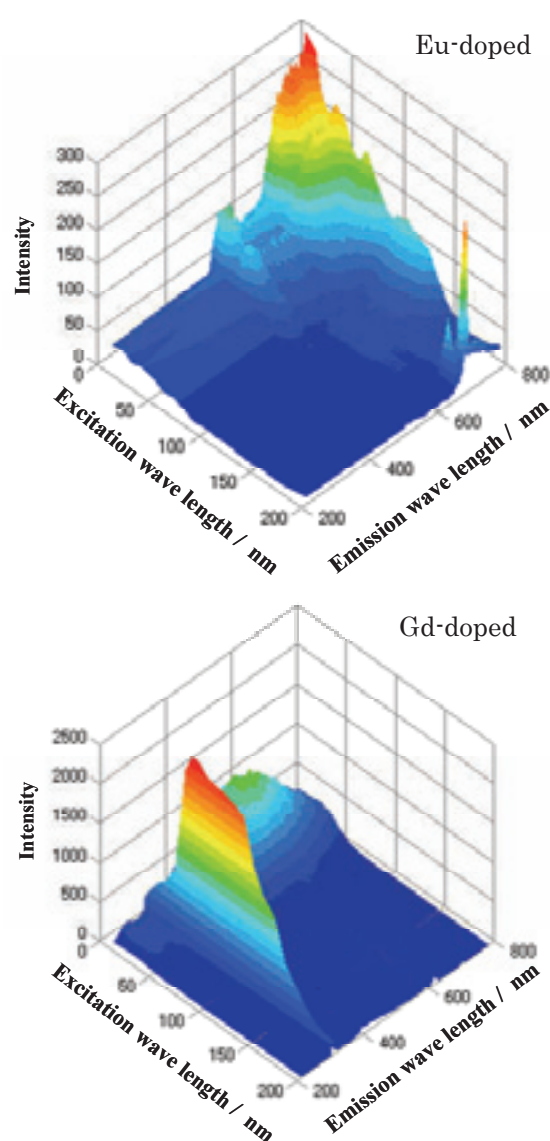


Fig. 1. These figures show the photoluminescent spectra of Eu ion or Gd ion-doped hydroxyapatite samples excited by ultraviolet synchrotron orbital radiation light.

## Field Effect on the Electronic States of Organic Thin Films: Incident Angle Dependence of Fluorescence-Yield XAS Spectra

H. S. Kato<sup>1</sup>, H. Yamane<sup>2</sup>, N. Kosugi<sup>2</sup> and M. Kawai<sup>1,3</sup>

<sup>1</sup>RIKEN (The Institute of Physical and Chemical Research), Wako 351-0198, Japan

<sup>2</sup>Institute for Molecular Science, Okazaki 444-8585, Japan

<sup>3</sup>Department of Advanced Materials Science, University of Tokyo, Kashiwa 277-8501, Japan

### Introduction

In order to extend new functionality of electronic devices, the molecular devices have recently been investigated with great efforts. The organic field effect transistor (OFET) is a typical molecular device that controls electric conductivity by injection of carriers into the organic thin film under the applied electric field. Since the organic materials consist of molecular units having their own molecular orbitals, it is not clear that the energy diagram of OFET is exactly the same as that of the inorganic semiconductors, i.e., band bending at the interface in the semiconductor side. Therefore, the direct observation of electronic states in the organic thin films under operative conditions has been required.

In our study, recently, *in situ* element-specific observation of electronic states of organic films beneath metal electrodes is successfully achieved by x-ray absorption spectroscopy (XAS) in the bulk-sensitive fluorescence yield (FY) mode, even under operational conditions. As a result, the bias dependence of the FY-XAS spectra of oligothiophene and pentacene films was detected. Since the obtained spectral changes have included an incomprehensive response, additional experiments were performed.

### Experimental

To investigate the electronic states of OFET, pentacene thin films on the SiO<sub>2</sub>-covered Si substrates were fabricated at RIKEN. We confirmed that the fabricated pentacene thin films show a *p*-type-like I-V property in the FET configuration. The pentacene films (35 nm thick) were covered homogeneously with a thin Au electrode (25 nm thick) to make uniform electric field in the films under the applied bias. The FY-XAS measurements were performed at the BL3U beamline of the UVSOR facility in IMS. The samples were set in a BL3U end-station through a sample-entry system. The fluorescence intensities were measured using a retarding field detector consisting of MCP plates.

### Results and Discussion

Figure 1 shows the incident angle dependence of the C K-edge FY-XAS spectra of the pentacene films, for which the spectra at the incidence angle of 0°, 30° and 60° from the surface normal were measured. At the measurements, the gate bias  $V_G$  was applied as a square wave (7 Hz) synchronized to two signal

counters for each of the top and bottom bias levels, which enabled us to get two different bias spectra in one photon energy sweep and to compare details of their spectra with sufficient reliability. In Fig. 1, the spectra at the bias of 0 V (blue lines) and -45 V (red lines) are plotted with their difference spectra (bold black lines). It is clear that the spectral changes from 0 V to -45 V increased with increasing incident angle.

In our previous studies, the bias dependence was observed at the normal incidence, so that the electric vector of the x-ray was perpendicular to the direction of the applied electric field. Since the spectral change is claimed to be a result of distorted molecular orbitals under the applied electric field, the previous experimental condition might not be sensitive to the orbital distortion. As the incident angle of the *p*-polarized x-ray increases, in contrast, the parallel component of the electric vector to the direction of applied electric field increases. Therefore, the increase of the difference signals with increasing incident angle, as shown in Fig. 1, rightly supports our previous deduction of the origin of the spectral change under applied bias.

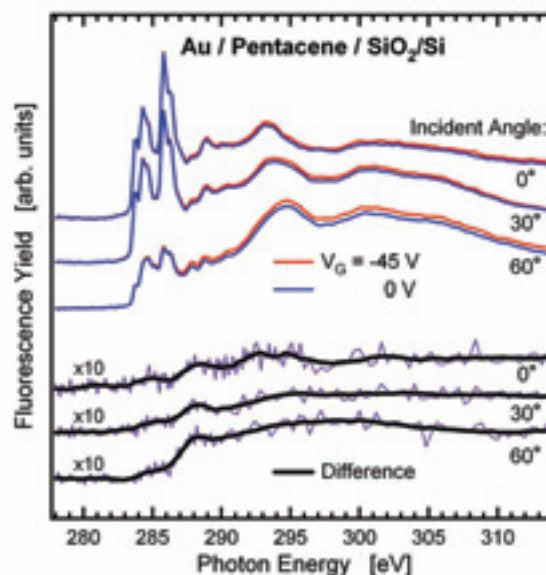


Fig. 1. Incident angle dependence of the C K-edge fluorescence-yield XAS spectra of the Au-covered pentacene films. The spectra were measured at the incident angle of 0°, 30° and 60° from the surface normal. Each set of the spectra at 0 V (blue line) and -45 V (red line) is plotted with their difference spectrum (bold black line).

## X-Ray Magnetic Circular Dichroism Study of Suppression of Iron Silicide Formation in Fe/Si<sub>3</sub>N<sub>4</sub>/Si(111)

K. Eguchi<sup>1</sup>, Y. Takagi<sup>1,2</sup>, T. Nakagawa<sup>1,2</sup> and T. Yokoyama<sup>1,2</sup>

<sup>1</sup>The graduate University for Advanced Studies (SOKENDAI), Okazaki 444-8585, Japan

<sup>2</sup>Institute for Molecular Science, Okazaki 444-8585, Japan

It is known that when transition metals are deposited on silicon substrates, metal silicides are easily formed, which are typically nonmagnetic materials. It is important to suppress the chemical interaction of transition metal atoms with Si substrates by modifying the Si substrate surface. An efficient method to provide well defined surfaces has not been reported so far. Previously, we tried to suppress iron silicidation using a Si(111)-( $\sqrt{3}\times\sqrt{3}$ )Ag substrate, but its effect is not sufficient to exhibit large magnetization [1]. In this work, we have measured Fe L-edge X-ray magnetic circular dichroism (XMCD) of Fe films on a Si<sub>3</sub>N<sub>4</sub>/Si(111)-(8×8) substrate.

The experiments were carried out at BL4B. Fe was deposited onto Si<sub>3</sub>N<sub>4</sub>/Si(111)-(8×8) and Si(111)-(7×7). The XMCD spectra were taken at  $H=\pm 5$  T and  $T=5$  K with the incident angles  $\theta$  of 0° and 55°. The helicity of the X-rays was fixed positively ( $P_c:0.41-0.60$ ), while the magnetic field was reversed.

Figure 1 shows magnetization curves of 1.6 ML Fe on Si<sub>3</sub>N<sub>4</sub>/Si(111)-(8×8) and Si(111)-(7×7), which were taken at the Fe L<sub>3</sub> peaks with the magnetic field normal to the surface. No magnetization can be seen in the Fe film on Si(111)-(7×7), because of the silicidation of iron atoms, while the Fe film on Si<sub>3</sub>N<sub>4</sub>/Si(111)-(8×8) was magnetized clearly. The fact indicates that the chemical interaction between Fe and Si atoms is suppressed effectively on the Si<sub>3</sub>N<sub>4</sub>/Si(111)-(8×8) substrate.

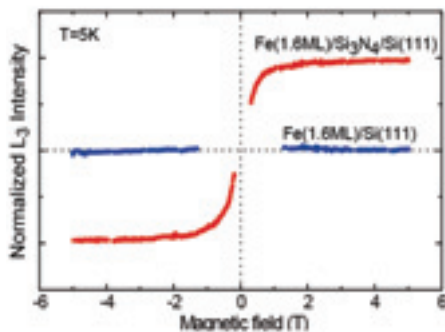


Fig. 1. Magnetization curves for Fe on clean Si(111) and Si<sub>3</sub>N<sub>4</sub>/Si(111). Both magnetic field and photon incident direction are perpendicular to the surface.

The spin and orbital magnetic moments were evaluated using the XMCD sum rule and the angle-dependent XMCD measurements. The magnetization of Fe on Si<sub>3</sub>N<sub>4</sub> was fully saturated under the condition of 5 T (See Fig.1). The angle-dependent XMCD spectra taken with the incident angles  $\theta$  of 0° and 55° are shown in Fig. 2. The spin magnetic moments of each thickness on the Si<sub>3</sub>N<sub>4</sub> surface are found to be much larger than that on the clean surface. Moreover, the spin magnetic moments increases monotonically with increasing the film thickness for the Fe/Si(111) system, because the Fe atom near surface does not form silicides in the thick film. On the other hand, that of the iron atom on Si<sub>3</sub>N<sub>4</sub> surface is 2.62  $\mu_B$  at 1.6 ML and the value decreases toward the bulk value of 2.2  $\mu_B$  with increasing the film thickness. It is revealed that the Fe atom deposited on the Si<sub>3</sub>N<sub>4</sub> surface does not react chemically with the Si atom.

In summary, the XMCD and M-H curves of iron were measured to evaluate the suppression effect of the iron silicide formation on the Si<sub>3</sub>N<sub>4</sub> surface. The silicidation of iron was found to be suppressed well using the Si<sub>3</sub>N<sub>4</sub> surface.

[1] Y. Takagi, K. Isami, I. Yamamoto, T. Nakagawa and T. Yokoyama, UVSOR ACTIVITY REPORT 37 (2010) 73.

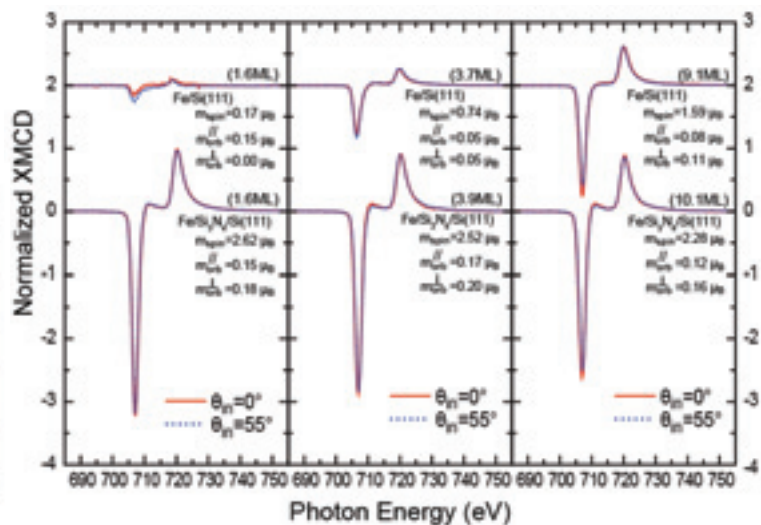


Fig. 2. XMCD spectra at L<sub>3,2</sub> edge of iron in Fe/Si(111) and Fe/Si<sub>3</sub>N<sub>4</sub>/Si(111) systems. Thickness is 1.6, 3.7, 9.1 ML and 1.6, 3.9, 10.1 ML, respectively. Applied magnetic field is 5 T and temperature of samples is 5 K. Incident angles of the light are 0° and 55° to normal direction of the surface.

## Magnetic Property of Iron Phthalocyanine on Co Films Studied by XMCD

Y. Takagi<sup>1,2</sup>, K. Eguchi<sup>2</sup>, T. Nakagawa<sup>1,2</sup> and T. Yokoyama<sup>1,2</sup>

<sup>1</sup> Institute for Molecular Science, Myodaiji-chio, Okazaki 444-8585, Japan

<sup>2</sup> The Graduate University for Advanced Studies, Okazaki 444-8585, Japan

In order to realize the molecular spintronic devices, it is crucial to understand the coupling between molecular spins and a magnetic metal surface. Metal phthalocyanines (Pc's) have attracted much interest due to their characteristic electronic and magnetic properties. Especially, iron(II) phthalocyanine (FePc) is one of these interesting and fundamental compounds because it takes the unusual intermediate triplet spin state and has large orbital moment. In this study, we report on the magnetic property of FePc on clean Cu(001) and magnetic Co layer grown on Cu(001) by means of X-ray magnetic circular dichroism (XMCD) at BL4B, which equipped with a super conducting magnet system.

Sample preparation and XMCD measurement were carried out in UHV chambers. A Cu(001) single crystal was cleaned by repeated cycle of Ar<sup>+</sup> sputtering and annealing. A Co layer was deposited on the clean Cu(001) at room temperature (RT). Purified FePc was deposited on these substrates at RT by sublimation and the thicknesses of the films were monitored by a quartz crystal oscillator. The intensity dependence of N K-edge X-ray absorption spectra (XAS) for the FePc film with X-ray incident angle indicated that the molecular was parallel to the substrate plane. The XAS and XMCD spectra were taken at 5 K and the XMCD spectra were recorded with reversal of magnetic field.

Figure 1 shows Fe L-edge XAS spectra of 25 ML FePc on clean Cu(001) and 1 ML FePc on Co(3ML)/Cu(001) at incident angle  $\theta = 55^\circ$ . The spectra of 25 ML film represent the electronic state of only FePc film because XAS is very surface sensitive. On the other hand, the shape of 1 ML FePc spectra is quite different from that of 25 ML FePc due to interaction between the FePc molecule and the Co layer.

The XMCD spectra of these films are showed in Fig. 2, which were taken at  $H = \pm 0$  T (remanence) and  $\pm 5$  T (saturation) and at temperature of 5 K. Both  $L_2$  and  $L_3$  XMCD signs of the 25 ML FePc film are negative, which indicates that the FePc film has a large orbital magnetic moment. In addition, the magnetic moments were detected in both films in remanence, which means that both films are ferromagnetic at 5 K. The remanent magnetization in the 1 ML FePc on Co layer is larger than that in the 25 ML FePc film on clean Cu(001). Additionally, magnetization curves measured for 1 ML FePc film on Co layer, which were recorded with Fe  $L_3$ -edge intensity for FePc films and with Co  $L_3$ -edge intensity for underlying Co layer, behaved similar dependence

with magnetic field. This result suggests the presence of a ferromagnetic exchange coupling between the Fe atom in the molecular and the Co atom in the underlying layer.

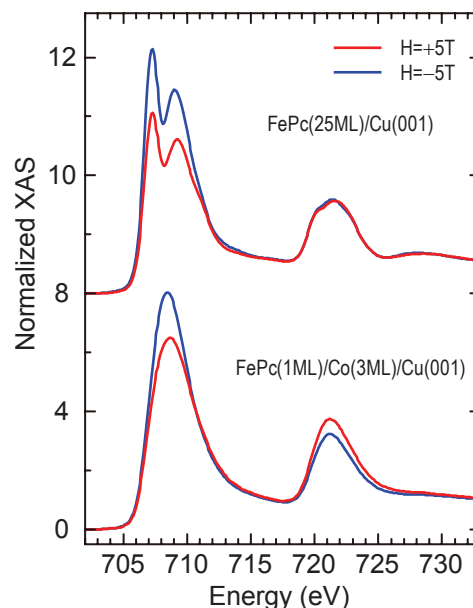


Fig. 1. Fe L-edge XAS spectra of 25 ML FePc on clean Cu(001) and 1 ML FePc on Co(3 ML)/Cu(001) at incident angle  $\theta = 55^\circ$  from the surface normal at  $H = 5$  T.

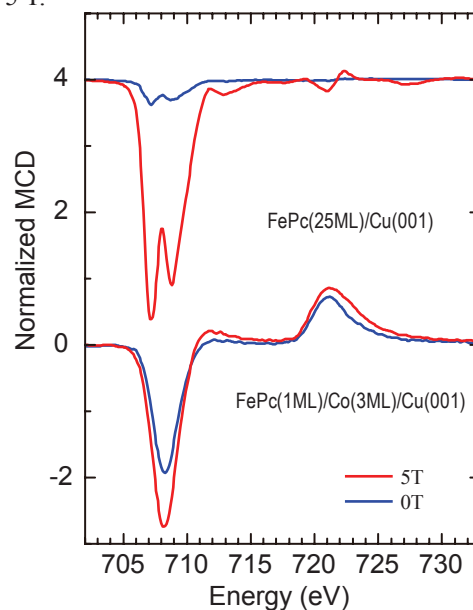


Fig. 2. Fe L-edge XMCD spectra of 25 ML FePc on clean Cu(001) and 1 ML FePc on Co(3 ML)/Cu(001) at incident angle  $\theta = 55^\circ$  from the surface normal.

## Electronic Structure of the Ferromagnetic Semiconductor EuO Ultrathin Films

H. Miyazaki<sup>1</sup>, T. Hajiri<sup>2</sup>, M. Matsunami<sup>1,3</sup>, T. Ito<sup>2</sup> and S. Kimura<sup>1,3</sup>

<sup>1</sup>UVSOR Facility, Institute for Molecular Science, Okazaki 444-8585, Japan

<sup>2</sup>Graduate School of Engineering, Nagoya University, Nagoya 464-8603, Japan

<sup>3</sup>School of Physical Sciences, The Graduate University for Advanced Studies, Okazaki 444-8585, Japan

Europium monoxide (EuO) is a ferromagnetic semiconductor with the Curie temperature ( $T_C$ ) at around 70 K [1, 2]. The magnetic moment originates from the half-filled  $4f$  shell of the  $\text{Eu}^{2+}$  ion with the spin magnetic moment of  $S = 7/2$ . Recently, we have revealed that the magnetism of EuO is caused by the hybridizations of the Eu  $4f - \text{O } 2p$  and Eu  $4f - 5d$  [3-5]. Applying EuO for spintronics devices such as spin filter tunnel barriers [3], it is important to investigate the physical properties as well as the electronic and magnetic structure of EuO thin films with a few nanometer-thicknesses. Three-dimensional angle-resolved photoemission spectroscopy (3D-ARPES) using synchrotron radiation is the most powerful technique to directly determine the electronic band structure. Using this technique, we observed the change of the electronic structure across  $T_C$ .

Single-crystalline EuO ultrathin films with thickness of about 2 nm were fabricated by a molecular beam epitaxy (MBE) method. Epitaxial growth of the single-crystalline EuO ultrathin films with the  $1 \times 1$  EuO (100) patterns was confirmed by a low energy electron diffraction (LEED) method.  $T_C$  was evaluated to be about 40 K by a magneto-optical Kerr effect (MOKE) *in-situ*. The 3D-ARPES measurements were performed at the beam line BL5U of UVSOR-II combined with the MBE system. The EuO ultrathin films grown in the MBE chamber and were transferred to a 3D-ARPES chamber under UHV condition. The total energy and momentum resolutions for the ARPES measurement were set to 45 meV and  $0.014 \text{ \AA}^{-1}$  at the X point ( $h\nu = 38 \text{ eV}$ ), respectively.

Figure 1 (a) shows the energy distribution curves (EDCs) of EuO (100) ultrathin film with a thickness of 2 nm near the X point at 5 K (ferromagnetic phase). From a comparison with the band calculation, the observed states at a binding energy  $E_B$  of 1.0 – 3.5 eV and 4.0 – 7.0 eV are attributed to the Eu  $4f$  and O  $2p$  states, respectively. From our previous results [5], the observed dispersive features of the Eu  $4f$  states around the X point indicates the hybridization of the Eu  $4f$  and O  $2p$  states, leading to the origin of the ferromagnetic phase transition of EuO. Figure 1 (b) shows the temperature dependence of the peak energies of the Eu  $4f$  states at the X point derived from the second-derivative EDCs. There are two Eu

$4f$  bands at the X point, which shift to the lower binding energy side on cooling across  $T_C$  of 40 K. The energy shifts of the higher binding energy peak are small compared to the bulk ones, corresponding to the decrease of  $T_C$ . This result indicates that the hybridization intensity between the Eu  $4f$  and other states becomes weaker with decreasing thickness. This result is consistent with our recent thickness-dependent band calculation.

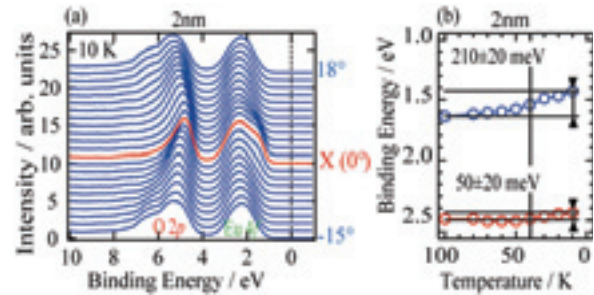


Fig. 1. (a) Energy distribution curves (EDCs) of an EuO (100) ultrathin film (2 nm thickness) near the X point. (b) Temperature dependence of the peak energies at the X point derived from the second-derivative EDCs of the Eu  $4f$  states.

- [1] N. Tsuda *et al.*, *Electronic Conduction in Oxides* (Springers College) (1976).
- [2] A. Mauger *et al.*, *J. Phys. (paris)* **39** (1978) 1125.
- [3] H. Miyazaki *et al.*, *Physica B* **403** (2008) 917.
- [4] H. Miyazaki *et al.*, *Jpn. J. Appl. Phys.* **48** (2009) 055504.
- [5] H. Miyazaki *et al.*, *Phys. Rev. Lett.* **102** (2009) 227203.
- [6] M. Müller *et al.*, *J. Appl. Phys.* **105** (2009) 07C917.

## Quantum Topological Phase Transition in Ultrathin Bi<sub>2</sub>Se<sub>3</sub> Films

Y. Sakamoto<sup>1</sup>, T. Hirahara<sup>1</sup>, H. Miyazaki<sup>2</sup>, S. Kimura<sup>2</sup> and S. Hasegawa<sup>1</sup>

<sup>1</sup>*Department of Physics, University of Tokyo, Tokyo 113-0033, Japan*

<sup>2</sup>*UVSOR Facility, Institute for Molecular Science, Okazaki 444-8585, Japan*

Topological insulators (TI) are a novel state of quantum matter in three dimensions (3D) that have been gaining increased attention. Along with its two-dimensional (2D) counterpart, the quantum spin Hall (QSH) phase, they are mathematically characterized by the so-called  $Z_2$  topological number [1]. While the bulk is insulating with an inverted gap, there is a metallic edge or surface state which is topologically protected and hence robust against weak perturbation or disorder.

One of the important aspect in the study of TI is the phase transition between the trivial (normal) and the topological state. The principal issue here is the exchange of the parity of conduction and valence bands by changing some external parameter. One example is the case of HgTe/CdTe quantum well. In this case, it was reported that by reducing the thickness of the well below a critical thickness of  $d_c = 60$  Å, the inverted band gap (band gap  $\Delta < 0$ ) once closes ( $\Delta = 0$ ) and becomes a normal band gap ( $\Delta > 0$ ) as schematically shown in Fig. 1 (a). Thus reducing the system size and changing the dimensionality does not only have the advantage that the surface-sensitivity is enhanced which will make the surface-state property more apparent in terms of 3D TI, but is also important in determining if the system is trivial or topological in 2D.

Bulk Bi<sub>2</sub>Se<sub>3</sub> is a 3D topological insulator with an inverted band gap and its surface states possess a linear band dispersion expressed by the Dirac equation [Fig. 1 (b)]. In a recent theoretical work, it was shown that this Hamiltonian possess similarity to the 2D QSH effective Hamiltonian for the HgTe quantum wells. The authors predicted that an energy gap will open in the surface-state dispersion due to the interaction between the top and bottom surfaces for thin film thicknesses. Furthermore, it was shown that the inverted gap will close at  $d_c = 25$  Å for Bi<sub>2</sub>Se<sub>3</sub>, and below  $d_c$  a normal band gap will develop so the system will become trivial [Fig. 1 (a)] [2]. Therefore a topological quantum phase transition is predicted to occur in the thin film limit. However this has not been experimentally demonstrated yet.

In the present study, we have performed angle-resolved photoemission spectroscopy (ARPES) measurements on ultrathin Bi<sub>2</sub>Se<sub>3</sub> films on silicon to verify if the phase transition actually takes place. Figure 2 shows the band dispersion for 2 (a), 3 (b) and 8 (c) quintuple layer (1 QL = 9.5 Å) ultrathin Bi<sub>2</sub>Se<sub>3</sub> films measured at the photon energy of 20 eV using circularly-polarized light. The band structure for the 8 QL film is similar to that found in bulk

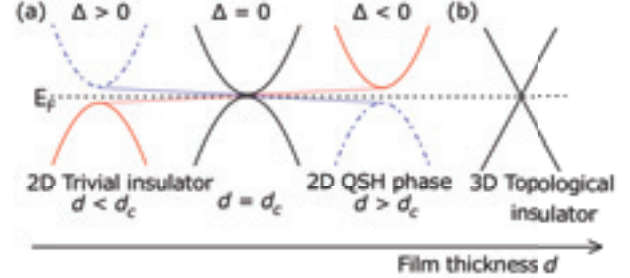


Fig. 1. Schematic drawing of the topological quantum phase transition in 2D. (b) Schematic drawing of the surface-state linear band dispersion of the 3D TI.

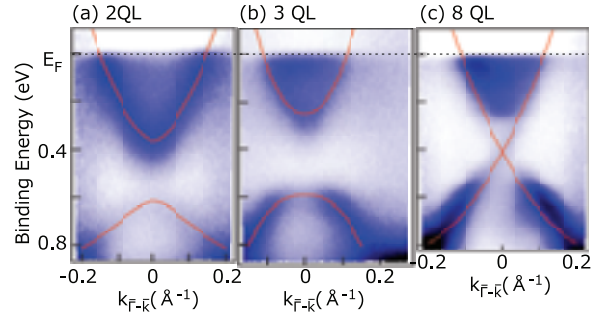


Fig. 2. E-k band dispersion images for the 2 QL (a), 3 QL, and 8 QL ultrathin Bi<sub>2</sub>Se<sub>3</sub> films along the  $\Gamma$ -K direction. The overlapped lines show the fitted curves using Eq. (1).

single crystals, showing the bulk bands just near the Fermi level as well as the Dirac surface states. On the other hand, the 2 and 3 QL films show a clear gap opening in the surface-state dispersion. However, the gap size is larger for the 3 QL film than the 2 QL one, which is counterintuitive to our understanding for particles confined in a potential, suggesting the occurrence of a parity reversal. Moreover, by fitting the measured images to (red solid lines in Fig. 2)

$$E_{\pm} = E_0 - Dk^2 \pm \sqrt{(v_F \hbar k)^2 + (\Delta/2 - Bk^2)^2}, \quad (1)$$

we are able to deduce the sign of  $\Delta$  and  $B$  which are related to the edge-state Hall conductance. This quantitative analysis also supported the occurrence of a transition from a QSH state (3 QL) to a trivial phase (2 QL). Thus we have found experimental evidence of a quantum topological phase transition in this system [3].

[1] L. Fu and C. L. Kane, Phys. Rev. B **76** (2007) 045302.

[2] H.-Z. Lu *et al.*, Phys. Rev. B **81** (2010) 115407.

[3] Y. Sakamoto *et al.*, Phys. Rev. B **81** (2010) 165432.

## Very Narrow Intermolecular Electronic Band Dispersion in a Crystalline Film of Zn-Phthalocyanine

H. Yamane and N. Kosugi

*Dept of Photo-Molecular Science, Institute for Molecular Science, Okazaki 444-8585, Japan*

The electronic band dispersion, energy *versus* wave vector  $E(\mathbf{k})$ , is a fundamental parameter to understand electric properties of solids such as hole mobility ( $\mu_h$ ). In the field of organic semiconductors, the study of the intermolecular  $E(\mathbf{k})$  shows a rapid progress due to the needs of the interpretation of the charge transport mechanism in molecular electronic devices. However, due to the very weak intermolecular interaction and the difficulty in preparing crystallized films sufficient for the  $E(\mathbf{k})$  measurement, the observation of the intermolecular  $E(\mathbf{k})$  has been limited to the case of high- $\mu_h$  materials. In order to elucidate and control the functionality of organic semiconductors, a systematic and quantitative experiment on the intermolecular interaction can play a crucial role. In this work, we have succeeded to observe a narrow intermolecular  $E(\mathbf{k})$  in crystalline films of Zn-phthalocyanine (ZnPc), which is one of the promising materials in the field of organic electronics. The present observation may pave the way for the systematic band structure analysis in the field of organic semiconductors.

The present experiment was performed using the angle-resolved photoemission spectroscopy (ARPES) system at BL6U. The crystallinity of the sample was confirmed by low-energy electron diffraction (LEED) and by the N K-edge X-ray absorption spectroscopy (XAS) in the sample-current mode. The  $E(\mathbf{k})$  relation was measured by ARPES at normal emission as a function of the incident photon energy ( $h\nu$ ), which scans the  $\mathbf{k}$  component along the surface normal. The sample temperature at all measurements was 15 K.

Figure 1 shows the incident angle ( $\alpha$ ) dependence of N K-edge XAS spectra for the 30-nm-thick films of ZnPc on Au(111). The sharp  $1s \rightarrow \pi^*$  transition peaks appear at  $h\nu = 398 \sim 405$  eV. These peaks are strongest at grazing incidence ( $\alpha = 60^\circ$ ) and are getting weaker with decreasing  $\alpha$ . Other broad  $1s \rightarrow \sigma^*$  transition features ( $h\nu > 405$  eV) show the opposite trend. From the data analysis, we found that the ZnPc film on Au(111) is well oriented with their molecular plane parallel to the substrate surface.

Figure 2 shows the  $h\nu$  dependent ARPES spectra at the normal emission for the ZnPc crystalline film on Au(111). Since the ZnPc crystalline film on Au(111) shows a Stranski-Krastanov growth mode, there are the remanent substrate signal such as a Fermi edge, which we used for the fine  $h\nu$  calibration. For the ZnPc-derived peaks A, B, and C, we have observed a clear dispersive behavior with  $h\nu$ , wherein (i) the periodicities of A–C are same in the  $\mathbf{k}$  space and (ii) the bandwidth of peak A, originating from the highest occupied molecular orbital (HOMO), is 120 meV.

The present observation clearly indicates that the band-like transport can be realized in phthalocyanine films by the control of the geometric film structure. Moreover, the present result can be a benchmark for the systematic study on the intermolecular interaction, e.g., intermolecular  $E(\mathbf{k})$  as a function of the central metal atom in the phthalocyanine molecule, which enables to discuss experimentally the intermolecular interaction in terms of the intermolecular distance and the molecular orbital symmetry.

The authors like to thank the staff of UVSOR, in particular, Mr. T. Horigome, Mr. E. Nakamura, and Prof. E. Shigemasa, for their fruitful assistance.

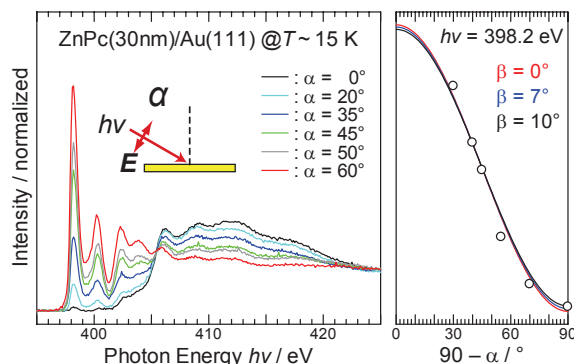


Fig. 1. The  $\alpha$  dependence of N K-edge XAS spectra for the crystalline ZnPc films on Au(111) at 15 K.

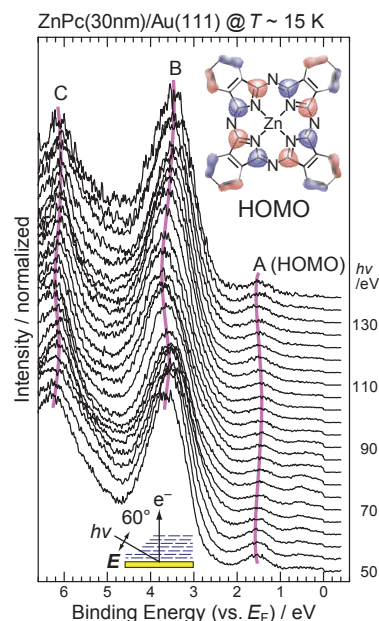


Fig. 2. The  $h\nu$  dependence of ARPES spectra (4 eV step) at the normal emission for the crystalline ZnPc films on Au(111) at 15 K.



## Interface Electronic Structure of Crownether-Derivatives on Cu(111)

H. Machida<sup>1</sup>, K. Yonezawa<sup>1</sup>, M. Yamamoto<sup>1</sup>, S. Hosoumi<sup>1</sup>, T. Hosokai<sup>2</sup>, T. Nishi<sup>3</sup>, N. Ueno<sup>1</sup>,  
and S. Kera<sup>1,3</sup>

<sup>1</sup>Graduate School of Advanced Integration Science, Chiba University, Chiba 263-8522, Japan

<sup>2</sup>Institut für Angewandte Physik, Universität Tübingen, Tübingen 72076, Germany

<sup>3</sup>Institute for Molecular Science, Okazaki 444-8585, Japan

Studies on the adsorption of large  $\pi$ -conjugated organic molecules on metal surfaces have increased considerable attentions, since the molecule/substrate interaction crucially influences electronic functions of organic devices. A missing study of the interface issue is on a molecular system with structural flexibility by  $sp^3$  bond ( $\sigma$  bond) in its main backbone. To reveal physical properties of such flexible molecules, we studied the valence electronic structure of tetrabromide-dibenzo-18-crown-6 (BDBC) thin films prepared on Cu(111) by using angle-resolved ultraviolet photoelectron spectroscopy (ARUPS).

### Experimental

ARUPS spectra were measured at photon incidence angle  $\alpha=60^\circ$ ,  $h\nu=28$  and 100 eV and  $T=295$  K. The molecules were evaporated onto the Cu(111). The monolayer (ML) formation was confirmed by the work function of the densely packed ML that shows a clear LEED pattern. High-resolution UPS spectra were also recorded using HeI light source.

### Results and Discussion

Figure 1 (a) shows the HeI UPS of BDBC(ML) on Cu(111) together with BDBC(ML)/HOPG and DOS by DFT calculation. The spectrum (1: thick curve) is shown after the background subtraction. All the bands of BDBC/Cu(111) are shifted to low-binding energy (Eb) side by 0.3-0.4 eV compared with BDBC/HOPG. Bands A (HOMO) and B seem to split on Cu(111)

due to strong coupling. An interface state (G) appears at the band-gap region.

Figure 1 (b) shows the UPS at Br(3d) region. Bands L and M are due to spin-orbit splitting and shifted to low-Eb side by 2.1 eV (bands L' and M') for BDBC(ML)/Cu(111), indicating Br atoms interact more strongly with Cu(111).

Figures 1 (c) and 1 (d) show ARUPS results for annealed-BDBC(ML)/Cu(111) along  $\Gamma$ -K direction. The photoelectron angular distributions (PAD) of split bands  $A_1$  and  $A_2$  are evaluated by curve fitting. These PAD patterns are different but show a nearly similar distribution, indicating both states could originate from the HOMO ( $\pi$  state distributed at phenyl rings) of a free BDBC and may split due to hybridization with the substrate, which may give differences in the  $\pi$ -MOs distribution. Moreover, the PADs have broad distribution around  $\theta=0$ - $30^\circ$ , leading the phenyl rings ( $\pi$  planes) are inclined to the substrate surface. All these show a clear evidence of chemisorptive interaction at BDBC/Cu(111) interface. An expected BDBC structure on Cu(111) is shown at the bottom of Fig.1 (d). The molecule-substrate distance and molecular deformation evaluated by x-ray standing wave measurements remarks a closer distance to the Cu(111) for Br atoms than other elements, which is consistent with the present UPS results.

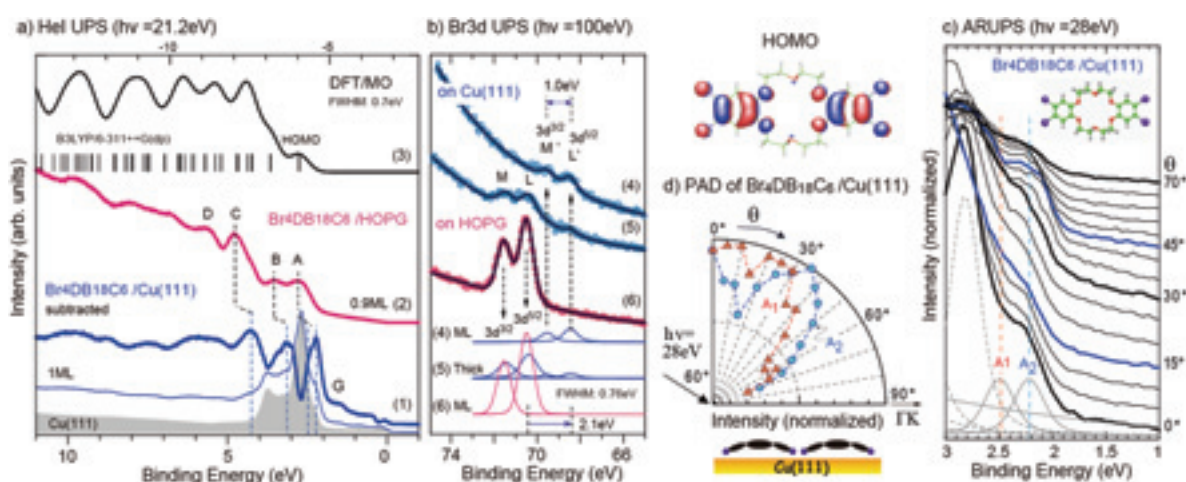


Fig. 1. (a) He I UPS of a clean Cu(111), BDBC(1ML)/Cu(111), and background subtracted BDBC(1ML) spectrum(1) together with BDBC(0.9 ML)/HOPG(2) and DFT-simulated spectrum(3). (b) Br(3d)-region UPS for 1ML/Cu(111)(4), thick-island film (7 nm)/Cu(111)(5) and 1ML/HOPG(6). Deconvoluted features in each spectrum are shown at the bottom. (c) ARUPS along  $\Gamma$ -K direction for BDBC(annealed ML)/Cu(111). (d) PAD for bands  $A_1$ (orange triangles) and  $A_2$ (blue circles). HOMO distribution on gas-phase and expected molecular conformation on Cu(111) are also shown.

## ARUPS Study of Pentacene Thin Film on Uniaxially Oriented PTFE Film

K. K. Okudaira, K. Ito, K. Hotta and N. Ueno

Association of Graduate Schools of Science and Technology, Chiba University,  
Chiba 263-8522, Japan

### Introduction

Electroactive organic molecules have attracted much attention owing to their versatility and unique electronic properties of interest for the design of optoelectronic and electronic devices. In-plane orientation of pentacene films has been performed in order to improve the transport properties in OFETs. Fabrication of oriented structure such as uniaxially oriented crystallites is important to obtain the oriented growth of materials as a substrate. The uniaxially poly(tetrafluoroethylene) (PTFE) films can be used as orienting media onto various substrate [1]. In this study, we observe angle-resolved ultraviolet photoelectron spectroscopy (ARUPS) and show the anisotropic orientation of pentacene (Pn) film on the uniaxially oriented PTFE thin films by evaporation onto the uniaxially polished Cu plate.

### Experimental

ARUPS measurements were performed at the beam line BL8B of the UVSOR storage ring at the Institute for Molecular Science. The take-off angle ( $\theta$ ) dependencies of photoelectron spectra were measured at incident angle of photon ( $\alpha$ ) =  $45^\circ$  with the photon energy ( $h\nu$ ) of 40 eV. At first (PTFE) was deposited on uniaxially polished polycrystal Cu plate by polishing paste (alumina particles with mean radius of about several  $\mu\text{m}$ ) (PTFE(5nm)/Cu). An additional organic layer of pentacene was subsequently evaporated to a final thickness of 10 nm on the uniaxially PTFE(5nm)/Cu (Pn(10nm)/PTFE(5nm)/Cu).

### Results and Discussion

Figures 1 (a) and (b) show the take-off angle ( $\theta$ ) dependencies of ARUPS spectra of Pn(10nm)/PTFE(5nm)/Cu with the parallel condition (the polarization plane of incidence photon is parallel to the polishing direction of Cu plate) and the perpendicular condition (the polarization plane of incidence photon is perpendicular to the polishing direction of Cu plate), respectively. The peak located at binding energy of about 1 eV corresponds to the localized  $\pi$  state (HOMO). Figure 2 shows the  $\theta$  dependence of photoelectron from HOMO band with the parallel and perpendicular condition. The  $\theta$  dependences with parallel condition have a sharp maxima at  $\theta = 65^\circ$ . On the other hand, with the perpendicular condition, the intensity of HOMO band does not show a strong  $\theta$  dependence. They indicate that the molecular orientation of pentacene film in parallel to polishing direction for Cu plate is different from that in

perpendicular to polishing direction. It was found that pentacene molecules show anisotropic molecular orientation on uniaxially oriented PTFE film.

[1] J. C. Wittmann et al., Nature **352** (1991) 414.

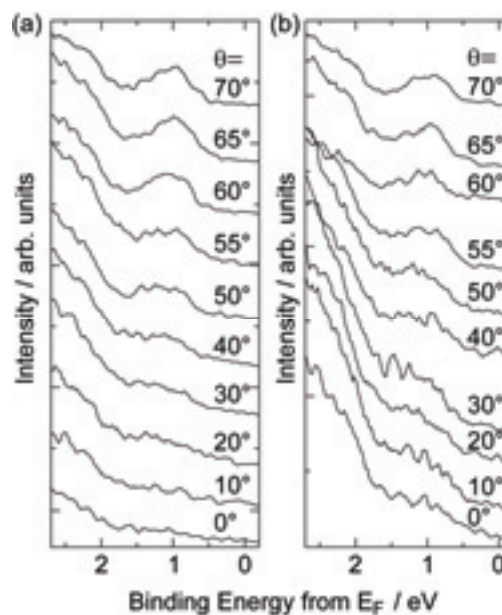


Fig. 1. Take-off angle ( $\theta$ ) dependencies of ARUPS of Pn(10nm)/PTFE(5nm)/Cu with (a) parallel and (b) perpendicular condition, respectively.

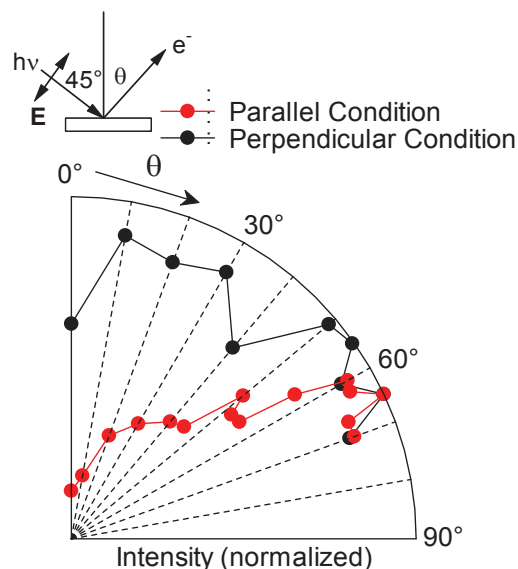


Fig. 2. Take-off angle ( $\theta$ ) dependencies of photoelectron intensities of HOMO peak of Pn(10nm)/PTFE(5nm)/Cu with parallel (●) and perpendicular condition (●).